Coral cover surveys corroborate predictions on reef adaptive potential to thermal stress

Oliver Selmoni[1,2], Gaël Lecellier[2,3], Laurent Vigliola[2], Véronique Berteaux-Lecellier[2], Stéphane Joost[1*]

1 - Laboratory of geographic information systems, Ecole Polytechnique Federale de Lausanne, Lausanne Switzerland
2 - UMR250/9220 ENTROPIE IRD-CNRS-Ifremer-UNC-UR, Labex CORAIL, Nouméa, New Caledonia
3 - UVSQ, Université de Paris-Saclay, Versailles, France
*=corresponding author

Abstract

As anomalous heat waves are causing the widespread decline of coral reefs worldwide, there is an urgent need to identify coral populations tolerant to thermal stress. Heat stress adaptive potential is the degree of tolerance expected from evolutionary processes and, for a given reef, depends on the arrival of propagules from reefs exposed to recurrent thermal stress. For this reason, assessing spatial patterns of thermal adaptation and reef connectivity is of paramount importance to inform conservation strategies.

In this work, we applied a seascape genomics framework to characterize the spatial patterns of thermal adaptation and connectivity for coral reefs of New Caledonia (Southern Pacific). In this approach, remote sensing of seascape conditions was combined with genomic data from three coral species. For every reef of the region, we computed a probability of heat stress adaptation, and two indices forecasting inbound and outbound connectivity. We then compared our indicators to field survey data, and observed that decrease of coral cover after heat stress was lower at reefs predicted with high probability of adaptation and inbound connectivity. Last, we discussed how these indicators can be used to inform local conservation strategies and preserve the adaptive potential of New Caledonian reefs.

1

Introduction

Coral bleaching is one of the main causes of severe declines of coral reefs around the world[1-3]. This phenomenon is mainly caused by anomalous heat waves leading to the death of hard-skeleton corals, which are the cornerstone of reefs[2]. Over the last 30 years mass coral bleaching events repeatedly struck worldwide, causing losses of local coral cover up to 50%[1,3]. In the coming years, bleaching conditions are expected to occur more frequently and to become persistent by 2050[4]. As up to one third of marine wildlife depends on coral reef for survival and at least 500 million people livelihoods worldwide[5], there is an urgent need to define new strategies to improve the preservation of these ecosystems[6].

Recent research reported reefs that rebounded from repeated heat stress and showed an increased thermal resistance[7–11]. Adaptation of corals against heat stress might explain such observations[12,13]. Under this view, identifying adapted coral populations is of paramount importance, as conservation strategies might be established to protect reefs hosting these corals from local stressors (e.g. via marine protected areas, MPAs)[14]. Furthermore, adapted corals could be of use in reef restoration plans and repopulate damaged reefs[15]. The adaptive potential of corals at a given reef depends on the arrival of propagules from reefs exposed to recurrent thermal stress[16,17]. This is why characterizing spatial patterns of thermal adaptation and reef connectivity is crucial to empower the conservation of the adaptive potential of corals[16,17].

Seascape genomics is a powerful method to evaluate spatial patterns of environmental variation and connectivity[17,18]. This method relies on a thorough analysis of environmental conditions around reefs using satellite data. Daily records of surface temperature are remotely sensed using satellites, and processed to compute indicators of thermal patterns associated with bleaching events[17,19,20]. Corals exposed to different thermal patterns are then sampled and genotyped to identify genetic variants correlated with these indicators[17,18]. The association between genetic variants and a given indicator defines a model of adaptation that can be used to predict the probability of adaptation, based on the value of the indicator itself[17,21]. In addition, by remote sensing sea current movements, it is possible to draw a connectivity map between every reef within an area of interest. This can be done using spatial graphs that resume multi-generational dispersal matching spatial patterns of genetic diversity in a given species[22]. This approach results in indices of connectivity defining, for a reef of

65   interest, the predisposition in sending (outbound connectivity) and receiving (inbound

66   connectivity) propagules to/from neighboring reefs[17].

67   In this study, we predicted spatial patterns of heat stress adaptation and connectivity for over

68   1000 km of coral reefs of New Caledonia, in the Southern Pacific (Fig. 1). The study area

69   encompassed the barrier reef surrounding Grande Terre, the main islands of the Archipelago,

70   as well as the intermediary and fringing enclosed in the lagoon. We also considered reefs

71   surrounding the Loyalty Islands (Ouvéa, Lifou and Maré) and the Astrolabe (east of Grande

72   Terre) and those in the Entrecasteaux and Petri atolls (north of Grande Terre). We first used

73   remote sensing data to (1) evaluate the thermal variability of the study area and (2) estimate

74   patterns of sea current connectivity between reefs. Next, we employed genomic data from a

75   seascape genomics study on three coral species of the region[23] in order to (1) compute the

76   probability of adaptation to heat stress across the whole region, and (2) verify whether

77   predicted reef connectivity matched genetic correlation between corals. Last, we compared

78   our predictions with field surveys of living coral cover recorded by the New Caledonian

79   observational network of coral reef (RORC; Job, 2018). Our results suggest that negative

80   effects of recent heat stress on coral cover are mitigated at reefs predicted with high

81   probability of heat stress adaptation and inbound connectivity. We then discuss the

82   conservation status of reefs around New Caledonia, and assess how conservation indices of

83   probability of adaptation and connectivity can be used to protect the adaptive potential of

84   corals of the region.

85

86

87

88

89

90

91

92

93

94

95

Figure 1. Reef system of New Caledonia. Coral reefs are highlighted in green. The blue dots correspond to sites of coral cover survey of the New Caledonian observational network of coral reef[24]. The red dots correspond to the sampling locations of coral specimen for the seascape genomics study that provide genetic data in the present study[23]. Sea regions highlighted in purple correspond to the marine reserves and protected areas as catalogued by the French agency for MPAs (http://www.aires-marines.fr/).
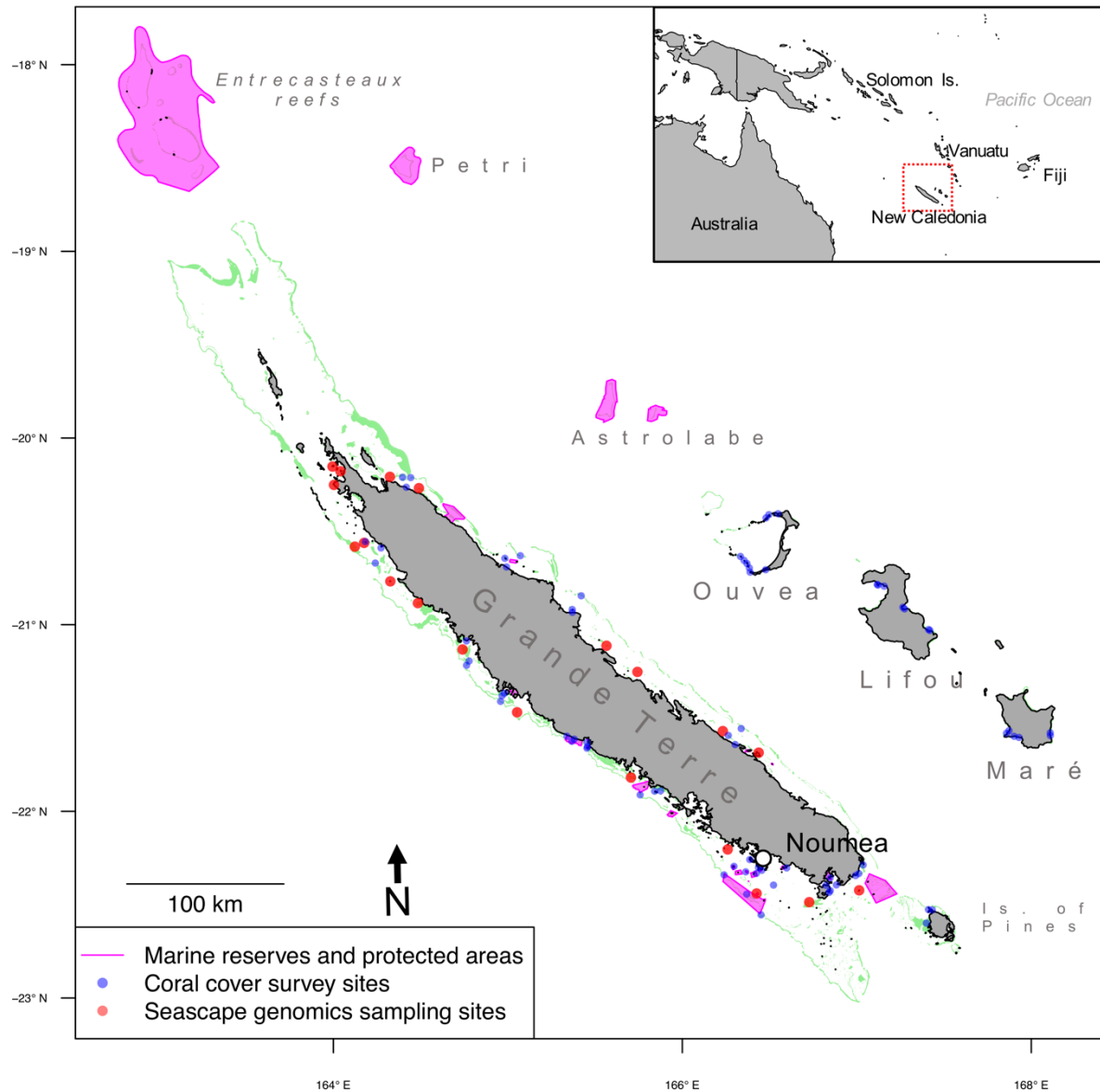
Results

Heat stress and probability of adaptation

The remote sensing data of sea surface temperature were processed to calculate the frequency of bleaching alert conditions (BAF$_{overall}$) across the reef system of New Caledonia (Fig. 2a). BAF$_{overall}$ was higher in reefs on the western coast of Grande Terre

106   (average BAF: 0.16±0.04) than in those on the eastern coast (0.08±0.03). Reefs in Lifou, Maré

107   and Isle of Pines displayed $BAF_{overall}$ values comparable to those on the eastern coast of

108   Grande Terre (0.09±0.03, 0.10±0.02 and 0.11±0.01, respectively), while in Ouvéa and

109   Entrecasteaux reefs the $BAF_{overall}$ values (0.15±0.01 and 0.12±0.01, respectively) were closer

110   to the values observed on the western coast.

111   Previous seascape genomics analyses on three corals of the region (*Acropora millepora,*

112   *Pocillopora damicornis and Pocillopora acuta*) revealed the presence of multiple genetic

113   variants (32 in total) potentially implicated in heat stress resistance[23]. We employed this data

114   to construct a logistic model of heat stress adaptation defining the probability of presence of

115   potentially adaptive variants (PA_{HEAT}) as a function of $BAF_{overall}$ (Fig. 2b). This model was then

116   used to produce a map of predicted PA_{HEAT} values for the whole region (Fig. 2c). It revealed

117   accentuated differences compared with $BAF_{overall}$ patterns, with PA_{HEAT} generally above 0.65

118   in reefs on the western coast of Grande Terre, Isle of Pines, Entrecasteaux and Ouvéa. In

119   contrast, values below 0.35 were observed at reefs located along the east coast of Grande

120   Terre, in Lifou and Maré.

121

122

123

124

125

126

127

128

129

130

131

132

133

134

135

136

Figure 2. Bleaching alert frequency and probability of heat stress adaptation. In (a), bleaching alert frequency ($BAF_{overall}$) is displayed for each reef of New Caledonia. This value is derived from remote sensing data of sea surface temperature, and describes the frequency of cumulated heat stress conditions that can lead to bleaching. In (b), a logistic model of heat stress adaptation is shown. This model is based on the frequencies of potentially adaptive genotypes of three coral species of New Caledonia[23]. The plot displays the probability of adaptation to heat stress as a logistic function of $BAF_{overall}$ (blue line, with the grey band showing the 95% interval of confidence). The model shown in (b) was used to translate $BAF_{overall}$ displayed in (a) in the probability of adaptation (PA_{HEAT}) against heat stress. The map in (c) displays PA_{HEAT} for every reef of New Caledonia.
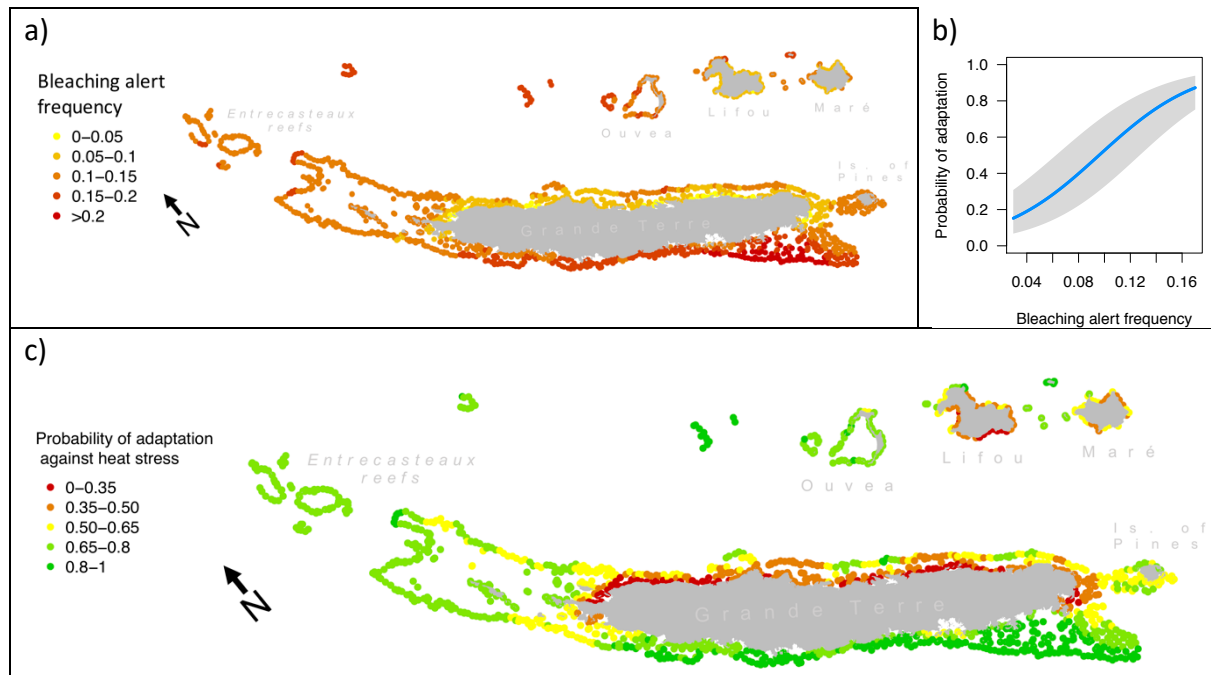
*Reef connectivity and genetic correlation between corals*

Remote sensing of sea current was used to compute a spatial graph of seascape connectivity predicting cost distances between reefs of New Caledonia. By using generalized linear mixed models (GLMMs) regression, we investigated whether such predictions on reef connectivity were representative proxies of the population structures of corals of the region. In three studied species (*A. millepora, P. damicornis* and *P. acuta*), we found that the genetic correlations between corals were significantly associated with the seascape cost distances separating the reefs where corals were sampled (*A. millepora*: p=1.46e-06; *P. damicornis*: p=1.63e-10 and *P.* acuta: p=6.7e-05; Fig. 3). This relationship was more stressed in the two *Pocillopora* species (regression coefficient for *P. damicornis*: $β$=-8.7E-05+ 1.4E-05; for *P. acuta*: $β$=-3.1E-05 ± 7.8E-06) than in *A. millepora* ($β$=-7.9E-06 ± 1.6E-06). The GLMMs accounted for the ancestral distance between pairs of individuals (*i.e.* the difference in

6

152 admixture from ancestral populations) which was found significantly associated to genetic

153 correlations between corals in all the three species (p~0; Fig. S1).

154

Figure 3. Seascape cost distance and genetic correlation between corals. The three plots display genetic correlations between pairs of corals sampled in New Caledonia as a function of the cost distance separating reefs where corals were sampled (blue line, with the grey band showing the 95% interval of confidence). Genetic correlations were computed as the correlation of single-nucleotide-polymorphisms, while seascape cost distance was predicted through seascape connectivity graphs. Each plot displays this association for a different species (a: *Acropora millepora*, b: *Pocillopora damicornis*, c: *Pocillopora acuta*).
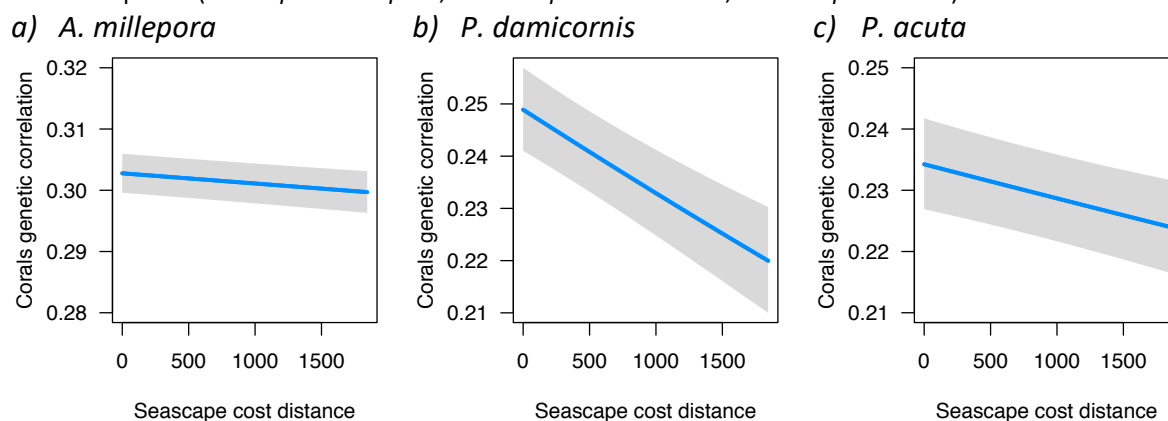

155

156 *Reef connectivity indices*

157

158 The seascape connectivity graph was used in the calculation of two indices describing the

159 dispersal characteristics of every reef of New Caledonia (Outbound Connectivity Index, OCI,

160 Fig. 4a; Inbound Connectivity Index, ICI, Fig. 4b). Both indices are expressed in km^2, as they

161 represent the area of the reefs neighboring a reef of interest. In OCI, neighboring reefs are

162 those potentially receiving propagules from the reef of interest, while in ICI neighboring reefs

163 are those potentially sending propagules towards the reef of interest.

164 Reefs that are more distant to Grande Terre (Entrecasteaux, Lifou, Maré and Ouvéa) had

165 lower OCI (average OCI: 202 ± 35 km^2, 410 ± 270 km^2, 210 ± 66 km^2, 864 ± 254 km^2, respectively;

166 Fig. 4a) than reefs surrounding Grande Terre. Reefs surrounding Grande Terre showed highest

167 values on the southern reefs of the eastern coast (1929 ± 300 km^2), while lower values were

168 predicted for the rest of the eastern coast (1377 ± 435 km^2) and the southern part of the

169 western coast (1119 ± 82 km^2). OCI was lower at reefs located at the northern extremity of

170 Grande Terre (632 ± 244 km^2).

171 Like with OCI, ICI was lower at reefs furthest from Grande Terre (Entrecasteaux, Ouvéa, Lifou,

172 Maré; average ICI of 460 ± 93 km^2, 177 ± 7 km^2, 97 ± 30 km^2, 111 ± 6 km^2, respectively; Fig. 4b).

7

173   ICI at reefs surrounding Grande Terre displayed a net contrast between the east and west

174   coasts, where ICI was lower on the east (498 ± 113 km^2) than the west (1287 ± 407 km^2).

175

Figure 4. Connectivitiy indices. Two connectvitiy indices based on sea current data are shown for every reef of New Caledonia. In a), the Outbound Connectivity Index (OCI) describes the predisposition in sending dispersal to neighboring reefs. In b), the Inbound Connectivity Index (ICI) summarizes the predisposition in receiving propagules from neighboring reefs. Both indices are given in km^2, as this represents the total surface of neighboring reefs.
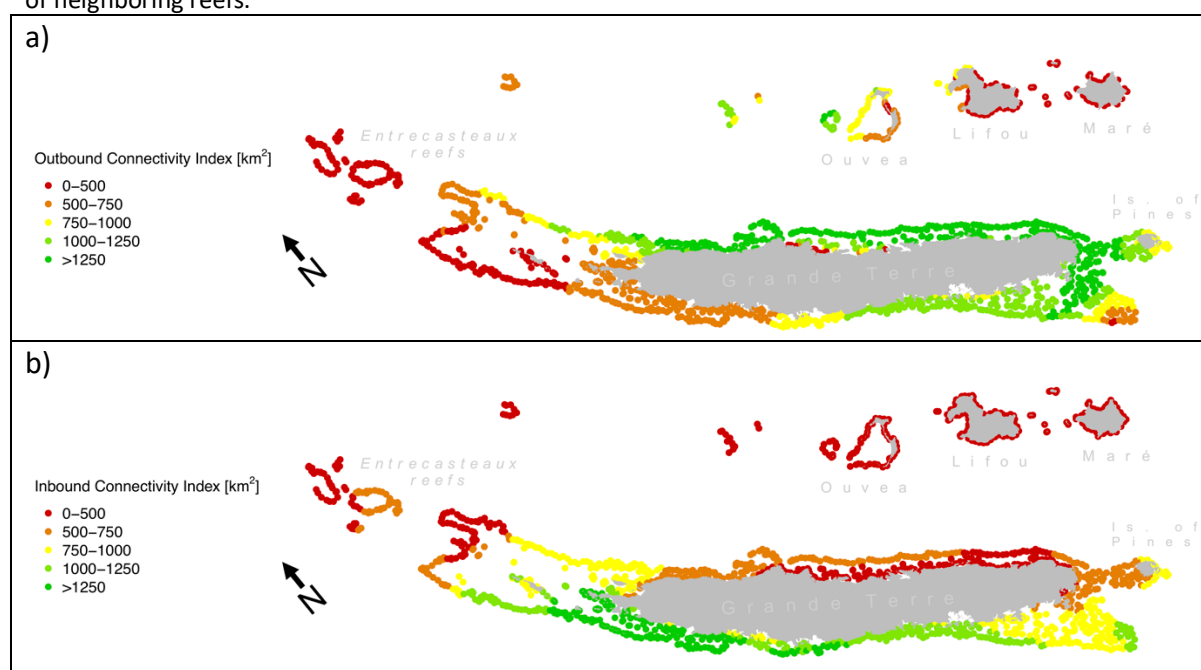
176

177   *Coral cover analysis*

178

179   Underwater surveys of New Caledonian reefs were analyzed to characterize the association

180   of living coral cover with recent thermal stress (BAF$_{previous\ year}$), probability of heat stress

181   adaptation (PA$_{HEAT}$) and connectivity indices (ICI and OCI; Fig. 5). We first investigated the

182   association between coral cover and individual explanatory variables using single fixed effect

183   GLMMs (Fig. 5a-d). We found that coral cover was significantly associated with BAF$_{previous\ year}$

184   (p=0.02), and that this association was of negative sign (β=-0.06$\pm$0.03; Fig. 5a). In contrast,

185   none of the other univariate models resulted in a significant association with coral cover

186   (PA$_{HEAT}$: p=0.93, Fig. 5b; OCI: p=0.46, Fig. 5c; ICI: p=0.41, Fig. 5d). The Akaike Information

187   Criterion (AIC) suggested a higher quality-of-fit for the model employing BAF$_{previous\ year}$ as

188   explanatory variable (AIC=-883), compared with the other univariate models (PA$_{HEAT}$: AIC=-

189   878; OCI: AIC=-879, ICI: AIC=-879).

190   We then investigated whether the negative association between coral cover and $BAF_{previous}$

191      $_{year}$ varied under different values of PA_{HEAT}, OCI or ICI. This analysis employed three bivariate

192   GLMM setting as fixed effects $BAF_{previous\ year}$ and the interaction between $BAF_{previous\ year}$ and

193   each of the three other explanatory variables (PA_{HEAT}, OCI, ICI; Fig. 5e-g). In comparison to all

194   the univariate models, those accounting for the interaction of $BAF_{previous\ year}$ with PA_{HEAT} and

195   ICI resulted in a higher quality-of-fit (AIC=-886 and AIC=-888, respectively). In both cases, the

196   effect of $BAF_{previous\ year}$ was significant (p<0.01) and of negative sign, whereas the effect of the

197   interaction was also significant but of positive sign (for the interaction with PA_{HEAT}:

198      $β$=+0.05±0.02, p=0.03; with ICI: $β$=+0.07±0.03, p=0.01; Fig. 5e-f). In contrast, the bivariate

199   model incorporating OCI had a quality-of-fit comparable to univariate models (AIC=-883), and

200   showed no significant association in interaction with $BAF_{previous\ year}$ (Fig. 5g).

201

Figure 5. Coral cover association analysis. The plots display the association of coral cover rates (blue line, with the grey band showing the 95% interval of confidence) with recent thermal stress ($BAF_{previous\ year}$), probability of heat stress adaptation (PA_{HEAT}) and connectivity indices (inbound connectivity index, ICI, and outbound connectivity index, OCI). In plots (a) to (d), the association with coral cover rates is shown for each explanatory variable alone (a: $BAF_{previous\ year}$, b: PA_{HEAT}, c: OCI, d: ICI). In the remaining plots, the association between coral cover and $BAF_{previous\ year}$ and is showed across different ranges PA_{HEAT} (e), OCI (f) and ICI (g).

202
203

10
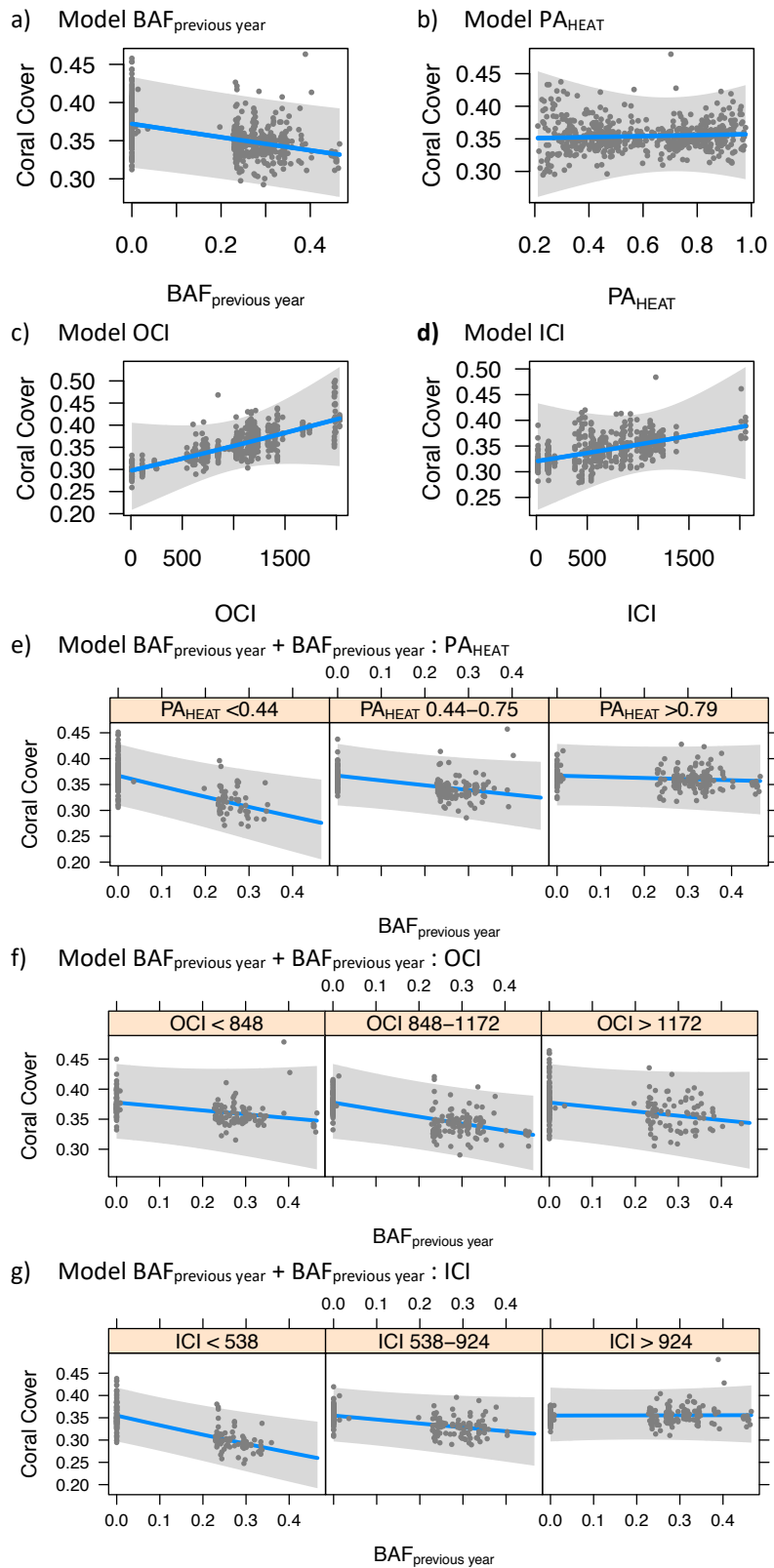
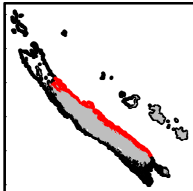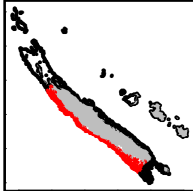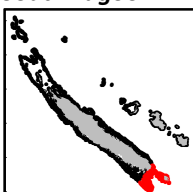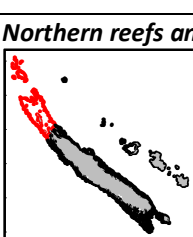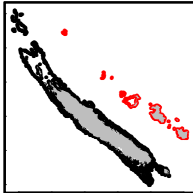**Discussion**

Local divergences in conservation indices

The metrics computed in this study stressed the strong asymmetry, in terms of both probability of heat stress adaptation (PA_{HEAT}) and connectivity (inbound connectivity index, ICI; outbound connectivity index; OCI), between reefs on the two coasts of Grande Terre (Fig. 2a, Fig.4). The climatic differences between the two coasts are modulated by the mountain range covering Grande Terre, and water conditions inside the lagoon reflect the combination of these differences coupled with oceanic influences[25]. For example, the southern part of the west coast of Grande Terre is subjected to coastal upwelling, a seasonal phenomenon bringing cold water to the surface[26]. While logic would suggest that cold water alleviates heat stress, research on the Great Barrier Reef in Australia showed that intense upwelling is followed by severe heat stress, and consequent coral bleaching[27]. While it is unknown whether this same effect occurs on the south-western coast of Grande Terre, this region does enclose the reefs that are predicted to experience the highest frequency of bleaching conditions across New Caledonia, and consequently to host corals with the highest PA_{HEAT} (Fig. 2).

Asymmetrical spatial patterns between the coasts of Grande Terre were also predicted for connectivity (Fig. 4), and this matched the genetic population structure of corals of the region (Fig. 3). In this work, we estimated connectivity using a straightforward approach, conceived to be reproduceable on any reef system around the world but that might lead to local inaccuracies[17]. However, our predictions were generally consistent with previous work that characterized the regional water circulation around New Caledonia using more sophisticated methods (i.e. combining oceanographic models, in situ measurements and shipboard detectors of sea currents)[28]. For instance, we observed a higher inbound connectivity index (ICI) on the west coast of Grande Terre (Fig. 4b), and a higher outbound connectivity index (OCI) on the east coast (Fig. 4a). This west-oriented connectivity was expected because of the South Equatorial Current crossing the archipelago in this direction[28]. This current bifurcates at the encounter of the New Caledonian shelf into 1) a weak and transient south-east oriented current between the Loyalty Islands and Grande Terre, and 2) a strong north-west oriented current flowing north of the Loyalty Islands[26,28,29]. This bifurcation explains the lower OCI observed in Lifou and Maré, compared with Ouvéa and the Astrolabe atolls. Last, the water

237 circulation inside the lagoon follows the north-west orientation of trade winds[26], resulting in

238 higher OCI in the south and higher ICI in the north.

239 Predictions of reef connectivity and PA_{HEAT} varied considerably across the different regions of

240 the study area (Fig. 2, 4), and conservation planning should account for these regional

241 peculiarities[14,31]. In table 1, we interpret the local divergences in values of PA_{HEAT}, ICI and OCI

242 under a conservation perspective.

243

Table 1. Implications for reef conservation in New Caledonia. The table describes the implications for reef conservation of the probability of heat stress adaptation (PA_{HEAT}), the outbound and inbound connectivity indices (OCI, ICI) predicted for different regions of the New Caledonia reef system. Information on the existing marine protected areas were retrieved from the French agency for MPAs (http://www.aires-marines.fr/).

East coast of Grande Terre	
	The east coast of Grande Terre hosts reefs predicted with low ICI and PA_{HEAT}. In contrast, OCI was generally higher than in the rest of the Archipelago. Reefs of strategic importance might be those located in the southern part as they had the highest OCI of the Archipelago, and also moderate levels of PA_{HEAT}. To date, only 4 km² of reefs in this area are protected. In addition, the establishment of nurseries with heat stress adapted corals might increase the adaptive potential of these reefs.
West coast of Grande Terre	
	Reefs on the west coast of Grande Terre generally displayed higher levels of ICI and PA_{HEAT}, compared with the rest of the Archipelago. Under an adaptive potential perspective, reefs in the northern part are of paramount importance as they receive the propagules from all the south-western reefs that experienced frequent heat stress. No MPA is established in this area. Another strategic region are the reefs in front of Noumea, in the southern part of the west coast, since they were predicted with high PA_{HEAT} and OCI. Here, more than 200 km² of protected areas are already established.
South Lagoon	
	The South Lagoon displayed heterogenous patterns of PA_{HEAT} and connectivity. The highest PA_{HEAT} were observed in the south-western extremity, which in turn was a region predicted with low OCI. The eastern part might be more interesting under a conservation perspective, as it was predicted with moderate PA_{HEAT} and high OCI. These reefs are located upstream of the trade winds, and can simultaneously send propagules to both coasts of Grande Terre. A large marine reserve (180 km²) is already established to protect these reefs. As for the southern part of the east coast, coral nurseries of heat stress adapted colonies might increase the adaptive potential of this region.
Northern reefs and Entrecasteaux reefs	
	Northern reefs and Entrecasteaux reefs were predicted with moderate to high levels of PA_{HEAT}, and low values of OCI and ICI, compared with the reefs around Grande Terre. The critical region under an adaptive potential perspective might be the eastern part of Northern reefs. This is because these reefs depend on the incoming propagules from the east coast of Grande Terre, which are predicted with low PA_{HEAT}.
Loyalty Islands, Astrolabe and Petri atolls	
	The main conservation issue for all the reefs in this region is the low ICI. It is likely that arrival of propagules substantially depends on the reefs from Vanuatu (Fig. 1), located ~200 km upstream on the South Equatorial Current. Reefs in Ouvéa and Astrolabe atolls (already protected) might be of strategic importance, as they were predicted with moderate to high values of PA_{HEAT} and OCI. Since reefs in Maré and Lifou showed low PA_{HEAT}, establishment of nurseries with heat stress adapted coral might be useful under an adaptive potential perspective.

244

Predictions on adaptive potential match coral cover

Heat exposure is considered to be one of the main drivers of coral mortality worldwide[11,32,33]. Our results were consistent with this view, as we found a significant negative association of coral cover with $BAF_{previous\ year}$ (Fig. 5a). Adaptation might contribute to increase thermal tolerance in corals, but its potential depends on two elements: the existence of adapted corals and the presence of reef connectivity patterns facilitating their dispersal. In this study, we found both of these elements (PA_{HEAT} and ICI) as associated with reduced loss of coral cover after thermal stress.

Previous studies have reported reefs that display increased thermal tolerance after recurrent exposure to heat stress[7–11], and recent research suggested that the thermal contrasts of New Caledonia might have driven adaptive processes in corals of the region[23]. Our results supported this view: while recent thermal stress ($BAF_{previous\ year}$) was associated with a reduction in coral cover, this reduction was mitigated at reefs that have experienced past thermal stress and were therefore predicted with high PA_{HEAT} (Fig. 5e). In addition, PA_{HEAT} alone did not result in a significant association with coral cover rates (Fig. 5b), and this might be due to the fact that thermal adaptation is advantageous only in response to heat stress. Indeed, previous research reported trade-offs in traits involved in local adaptation and acclimatization to heat stress in corals [34]. These trade-offs might explain why the highest rates of coral cover (>0.4) in absence of heat stress ($BAF_{previous\ year}$=0) were mainly observed at reefs with low PA_{HEAT} (Fig. 5e).

Outbound connectivity was not found to be associated with changes in coral cover (Fig. 5c,f). This is not surprising, because beneficial effects of dispersal are expected at reefs receiving incoming propagules, rather than the opposite [16,35]. Indeed, inbound connectivity was found to mitigate the negative association between $BAF_{previous\ year}$ and coral cover (Fig. 5g). Two non-mutually exclusive reasons might explain this observation. First, high levels of incoming propagules might facilitate the turnover of dead colonies caused by heat stress[36], although it has to be noted that this kind of recovery usually requires several years [37]. Second, incoming dispersal facilitates the arrival of adapted propagules, and therefore promotes an adaptive response even at reefs that did not experience thermal stress before[38]. Indeed, we observed that the frequency of adaptive genotypes in *A. millepora* and *P. acuta* was generally higher at reefs predicted with low PA_{HEAT} and high ICI, than in those predicted with both low PA_{HEAT} and

277 low ICI (Fig. S2). This view on genetic rescue via incoming migration is supported by the fact

278 that every reef depends, to some extent, on its neighbors for larval recruitment[39].

279

280 *Limitations and future directions*

281

282 The associations found between changes in coral cover and the descriptors of thermal stress,

283 probability of heat stress adaptation and connectivity do not necessarily imply causative

284 relationships. Despite evidence of effects of thermal patterns on coral cover reported by

285 previous studies, there might be other environmental constraints that are asymmetrical

286 between the two coasts of Grande Terre and modulate coral cover changes. Further

287 validation remains necessary and could be achieved via experimental assays of heat stress

288 resistance[8] in colonies sampled at reefs with different PA_{HEAT}. This approach would also

289 enable disentangling of the possible confounding role of acclimatization in heat stress

290 adaptive responses [12,34].

291 Another important aspect to consider in future studies is the resolution of remote sensing

292 datasets used for predictions. Here, we worked at a resolution of ~5 km for thermal variables

293 and ~8.5 km for sea current data. While the overall environmental patterns appeared

294 consistent with those characterized in previous studies, it is likely that small scale phenomena

295 were neglected. For instance, reef heat stress exposure can vary substantially under the fine-

296 scale (<1km) of a seascape[13]. The same applies to connectivity, since the use of high resolution

297 (≤1 km) hydrodynamic models could improve the characterization of coral larvae fine-scale

298 dispersal[40,41].

299 A third limitation of our approach concerns the generalization of the biological and ecological

300 characteristics of a reef. Here we assumed that the reef system of New Caledonia was a single

301 homogenous ecological niche, hosting an "average" species with an "average" heat stress

302 adaptive response. This simplification is useful to portray an overall prediction, but might lead

303 to local inaccuracies. This is because the reef types of New Caledonia are variegated and

304 species distributions varies accordingly[42,43]. Furthermore, different species have different

305 levels of bleaching sensitivity[44] and reproduce under different strategies[45]. For instance, the

306 propagules of a broadcast spawning coral as *A. millepora* travel over longer distances,

307 compared with those of brooding species as *P. damicornis* and *P. acuta*[30]. Consequently, *A.*

14

308   *millepora* showed a lower rate of decrease of genetic correlation between corals per unit of

309   seascape cost distance, in comparison with the *Pocillopora* species (Fig. 3).

310   In future studies, PA$_{HEAT}$ and connectivity predictions should be calibrated to match these

311   biological differences. It is for this reason that seascape genomics studies will become of

312   paramount importance into the future, as they provide species-specific indications on 1) how

313   thermal stress might be translated in probability adaptation, and 2) the biological meaning

314   (e.g. degree of genetic separation) of a cost distance by sea currents[17,18].

315
316   *Conclusions*
317
318   In this study, we combined remote sensing of environmental conditions with genomic data

319   to predict spatial patterns of heat stress adaptation and connectivity for the coral reefs of

320   New Caledonia. We then retrieved field survey data and showed that recent heat stress was

321   associated with a decrease in living coral cover, but also that such association appeared to be

322   mitigated at reefs predicted with 1) high probability of heat stress adaptation and 2) high

323   levels of incoming dispersal. The metrics computed in this work resumes the adaptive

324   potential of corals against heat stress, and therefore represents valuable indices to support

325   spatial planning of reef conservation.

326

327

328   **Methods**

329
330   *Remote sensing of sea surface temperature*

331

332   Satellite data characterizing sea surface temperature (SST) were retrieved from a publicly

333   available database (dataset: ESA SST CCI reprocessed sea surface temperature analyses)[46,47].

334   This dataset provides daily records of SST at a ~5 km resolution from the years 1981 to 2017

335   across the whole study area (Fig. 1). The shapes of the reef of the region[48] were transformed

336   into a regular grid (1,284 cells with maximal size of 5x5 km), and for each reef cell we extracted

337   the average temperature for every day of the observational period using QGIS software[49].

338   We performed calculations of heat stress patterns in the R environment using the *raster*

339   package (v. 3.0)[50,51]. For each reef cell, patterns of heat stress were computed using the

340   bleaching alert definition developed by the Coral Reef Watch briefly described hereafter[20].

341   For every day, we calculated the "hotspot value" as the difference between SST and the

342   maximal monthly mean (MMM, usually the monthly average of February in New Caledonia).

343   The hotspot value was retained only when SST exceeded the MMM by at least 1 °C. Next, for

344   each day, we calculated the cumulated hotspot values over the previous 84 days (3 months),

345   and if this sum is > 0, the day is flagged as being 'under bleaching alert'. Finally, we computed

346   the frequency of days under bleaching alert for every year (BAF_{year}) from 1985 to 2017. For

347   the preceding years (1981-1984), BAF_{year} was not calculated such to avoid bias caused by

348   estimating MMM over a limited number of years. An overall measure of BAF ($BAF_{overall}$) was

349   calculated as the average of all the BAF_{year} from 1985 to 2017.

350

351

352   *Seascape connectivity graph*

353

354   For the estimation of connectivity we applied a method based on spatial graphs previously

355   employed to study coral reef connectivity[17] and briefly outlined hereafter. We retrieved a

356   publicly available dataset describing the eastward and northward surface water velocity

357   (Global Ocean Physics Reanalysis)[46]. This dataset provided daily records at ~8.5 km resolution

358   from 1993 to 2017. Since this resolution can be inaccurate close to coastlines, we increased

359   the resolution to 1 km using the "resample" function ("bilinear" method) of the *raster* R

360   package, and used high resolution bathymetry data (100 m resolution[52]) to remove the sea

361   velocity value from pixels located on land. We then used the R package *gdistance* (v. 1.2)[53] to

362   create a matrix describing the transition costs between each adjacent pixel in the study area.

363   These costs were inversely proportional to the frequency of transition based on sea currents.

364   This seascape connectivity graph was calculated as the shortest cost distances across this

365   matrix between for each pair of the 1,284 reef cells. Of note, two least-cost-paths were

366   calculated for each pair of reef cells, one for each direction of the transition.

367

368   *Connectivity indices*

369

370   The seascape connectivity graph was used to compute two indices connectivity for every reef

371   cell of the study area: inbound connectivity and outbound connectivity. These indices had

372   been defined in previous work on corals[17] and were calculated in the R environment.

373   *- Outbound connectivity index (OCI)*: represents the predisposition of a reef to send coral

374   propagules to its neighbors. For a given reef cell, it is calculated by defining all the neighboring

375   reef cells that can be reached under a determined cost distance threshold (CDt). OCI is the

376   total area (in km^2) of the destination reef cells.

377   *- Inbound connectivity index (ICI)*: represents the predisposition of a reef to receive coral

378   recruits from its neighbors. For a given reef cell, it is calculated by defining all the neighboring

379   reef cells that can reach this target reef cell under a determined CDt. ICI is the total area (in

380   km^2) of these departure reef cells.

381   We set the value of CDt to 800 units in order to maximize the neighborhood without causing

382   border effects. This value was calculated based on the reef cells' cost distance to and from

383   the borders of the study area (located ~250 km around the most peripheral reef cells), where

384   the minimal cost distances to and from the border were 836 and 801 units, respectively.

385

386   *SNPs dataset*

387

388   We retrieved genomic data employed in previous seascape genomics analyses on three coral

389   species of New Caledonia: *Acropora millepora, Pocillopora damicornis* and *Pocillopora*

390   *acuta*[23]. This dataset encompassed more than one hundred individuals per population (167

391   in *A. millepora,* 118 in *P. damicornis*, 110 in *P. acuta*), collected at multiple sampling sites

392   around Grande Terre (20 sites for *A. millepora,* 17 for *P. damicornis*, 17 for *P. acuta*) and

393   genotyped using a Genotype-By-Sequencing approach[54] characterizing thousands of single-

394   nucleotide-polymorphisms (SNPs; 11,935 in *A. millepora*, 7,895 in *P. damicornis* and 8,343 in

395   *P. acuta*). Of note, SNPs in this dataset were already filtered for rare allelic variants (minor

396   allele frequency<0.05%) and linkage disequilibrium (LD-pruning threshold=0.3[55]).

397

398   *Probability of heat stress adaptation*

399

400   The previous seascape genomics study investigated the genotype-environment associations

401   between SNPs and 47 environmental descriptors (among which is BAF$_{overall}$) using LFMM

402   software[23,56]. In each of the three species, the analysis reported significant associations

403   (q<0.01) of BAF$_{overall}$ with potentially adaptive SNPs (10 in *A. millepora*, 18 in *P. damicornis,*

404   and 4 in *P. acuta*). We employed these genotype-environment associations to predict the

405   probability of heat stress adaptation (PA$_{HEAT}$) from BAF$_{overall}$ values. We used a method based

406   on logistic regressions[21,57] that was previously applied to corals[17], with some modifications

407   outlined hereafter.

408   For each individual used in the analysis, we retrieved the BAF$_{overall}$ value at the sampling

409   location. Next, we encoded the presence/absence of the putatively adaptive genotype as a

410   binary variable using a custom function in the R environment. We then employed a generalize

411   linear mixed model (GLMM) to evaluate how the presence/absence of putative adaptive

412   genotypes (response variable) responded to BAF$_{overall}$ (explanatory variable) across all the

413   selected SNPs, individuals and species combined. This was done through the R package

414   glmmTMB (v 1.0)[58], using a logistic regression model where SNP identifier, sample identifier

415   and species were introduced as random factor. The resulting model then was used to

416   transform BAF$_{overall}$ values associated with each of the 2,284 reef cells of New Caledonia in

417   PA$_{HEAT}$. The model was plotted using the visreg R package (v. 2.6.1)[59].

418

419   *Reef connectivity and genetic correlations between corals*

420

421   The SNPs dataset was used to evaluate whether reef connectivity predictions were

422   representative proxies of the structure of three coral populations. In the R environment, we

423   applied the following framework to the genotype matrix of each of the three species. First,

424   we evaluated the relatedness between each pair of individuals in the dataset (13,861 pairs in

425   *A. millepora*, 6,903 pairs in *P. damicornis*, 5,995 pairs in *P. acuta*) by calculating the genetic

426   correlation (Pearson) based on SNPs values[60,61]. We then computed the distribution of the

427   genetic correlation values, and excluded pairs of individuals with anomalously high or low

428   correlation (*i.e.* exceeding the boundaries defined by the median of the distribution ± three

429   times the interquartile range).

430   Next, we investigated the drivers of genetic correlations by using GLMMs designed through

431   the R package glmmTMB[58]. We set two fixed effects as possible drivers of genetic correlation

432   between individuals: ancestral distance and reef connectivity. Accounting for ancestral

433   genetic structure is particularly important as corals are prone to hybridization or cryptic

434   speciation[62,63]. The computation of ancestral distance featured the R package ALStructure (v.

435   0.1)[64]. For a given SNP matrix, ALStructure predicts the number of ancestral populations, and

436   then estimates, for every individual, the admixture proportions to the ancestral populations.

437 For every pair of individuals, we then calculated the ancestral distance as the Euclidean

438 distance between the respective admixture proportions. For which concerns reef

439 connectivity, the fixed effect corresponded to the least-cost-path (from the seascape graph)

440 linking the sampling sites of every pair of individuals. Since genetic correlations could not

441 exceed the 0-1 boundaries, GLMMs were built using a beta regression[65]. The random factors

442 in the GLMM were the identifiers of the individuals in the pairs, as well as the identifier of the

443 pair of sampling sites.

444 Finally, we evaluated the relationship between ancestral distance, reef connectivity and

445 genetic correlations of corals by 1) reporting the estimate and its standard deviation, as well

446 as the p-value associated with Wald statistic[58]; 2) plotting the association using the visreg R

447 package[59].

448

449 *Coral cover data*

450

451 Living coral cover data was retrieved from the 2017-18 report of the New Caledonian

452 observational network of coral reefs ('Réseau d'observation des récifs coralliens de Nouvelle

453 Calédonie', RORC; Job, 2018). Overall, we used data from 74 survey stations distributed across

454 the Archipelago of New Caledonia (Fig. 1). At each station, yearly coral cover surveys were

455 performed along the same 100m transect using the "point intercept" technique. Surveys

456 covered the period from 2003 to 2017, where 18 sites have been visited for less than five

457 years, 27 for five to ten years, and 29 for more than ten years. The exact coordinates of survey

458 stations were retrieved from the geographic information web-portal of New Caledonia

459 (https://georep.nc/).

460

461 *Environmental characterization of survey sites*

462

463 The coordinates of survey stations were used to find the corresponding reef cells and the

464 associated values of the connectivity indices (OCI and ICI). For each survey record (i.e. survey

465 at a given station in a specific year) we also calculated $BAF_{overall}$ as the average BAF since 1985

466 to the year proceeding the survey. Based on the values of $BAF_{overall}$ we computed PA_{HEAT} for

467 each survey record. In addition, we calculated BAF values on a rolling temporal window

468 describing average BAF for the year ($BAF_{previous\ year}$) that preceded the year of survey.

469

470   *Analysis of coral cover change*

471

472   We investigated the association of $BAF_{previous\ year}$, PA_{HEAT} and connectivity indices (ICI and OCI;

473   in total 4 explanatory variables) with coral cover rates (response variable) using GLMMs. This

474   analysis focused on the coral cover rates of every survey record (total of 574 records). The

475   computation of GLMMs was performed using the R package glmmTMB (v 1.0)[58], which

476   allowed us to model coral cover rates via beta regression [65]. We accounted for the non-

477   independence of survey records originated at the same station but on different years by

478   setting the station effect as random factor on the coral cover rate[66]. This approach is

479   recommended for studies of longitudinal data with irregular time points[67]. To avoid bias due

480   to scale differences between explanatory variables, each variable was standardized to mean

481   0 and standard deviation 1 using the R "scale" function.

482   We built two types of GLMMs: univariate and bivariate. In univariate GLMMs, $BAF_{previous\ year}$,

483   PA_{HEAT}, ICI and OCI were employed each as unique fixed effect. The goal was to determine

484   whether the explanatory variables showed a standalone association (*i.e.* independent from

485   other variables) with coral cover change. In bivariate models, GLMMs were constructed each

486   with two fixed effects: 1) $BAF_{previous\ year}$ and 2) the interaction between $BAF_{previous\ year}$ and each

487   of the remaining explanatory variables: PA_{HEAT}, ICI and OCI. The goal of bivariate models was

488   to investigate whether the potential effect of recent thermal stress ($BAF_{previous\ year}$) on coral

489   cover might be modulated by PA_{HEAT}, ICI or OCI.

490   For each GLMM, we reported the estimate and its standard deviation, as well as the p-value

491   (deemed significant when <0.05) associated with Wald statistic[58] of the fixed effects. In

492   addition, we compared the quality-of-fit of models by calculating the Akaike Information

493   Criterion (AIC)[68].

494

495   **Acknowledgments**

496

502

503

References

1. Hughes, T. P. *et al.* Global warming and recurrent mass bleaching of corals. *Nature* **543**, 373–377 (2017).

2. Bellwood, D. R., Hughes, T. P., Folke, C. & Nyström, M. Confronting the coral reef crisis. *Nature* **429**, 827–833 (2004).

3. Hughes, T. P. *et al.* Spatial and temporal patterns of mass bleaching of corals in the Anthropocene. *Science (80-.).* **359**, 80–83 (2018).

4. Van Hooidonk, R., Maynard, J. A. & Planes, S. Temporary refugia for coral reefs in a warming world. *Nat. Clim. Chang.* **3**, 508–511 (2013).

5. Costanza, R. *et al.* Changes in the global value of ecosystem services. *Glob. Environ. Chang.* **26**, 152–158 (2014).

6. Moberg, F. & Folke, C. Ecological goods and services of coral reef ecosystems. *Ecol. Econ.* **29**, 215–233 (1999).

7. Hughes, T. P. *et al.* Ecological memory modifies the cumulative impact of recurrent climate extremes. *Nature Climate Change* **9**, 40–43 (2019).

8. Krueger, T. *et al.* Common reef-building coral in the northern red sea resistant to elevated temperature and acidification. *R. Soc. Open Sci.* **4**, 170038 (2017).

9. Penin, L., Vidal-Dupiol, J. & Adjeroud, M. Response of coral assemblages to thermal stress: are bleaching intensity and spatial patterns consistent between events? *Environ. Monit. Assess.* **185**, 5031–5042 (2013).

10. Thompson, D. M. & van Woesik, R. Corals escape bleaching in regions that recently and historically experienced frequent thermal stress. *Proc. Biol. Sci.* **276**, 2893–2901 (2009).

11. Sully, S., Burkepile, D. E., Donovan, M. K., Hodgson, G. & van Woesik, R. A global analysis of coral bleaching over the past two decades. *Nat. Commun.* **10**, 1–5 (2019).

12. Thomas, L. *et al.* Mechanisms of Thermal Tolerance in Reef-Building Corals across a Fine-Grained Environmental Mosaic: Lessons from Ofu, American Samoa. *Front. Mar. Sci.* **4**, 434 (2018).

13. Bay, R. A. & Palumbi, S. R. Multilocus adaptation associated with heat resistance in reef-building corals. *Curr. Biol.* **24**, 2952–2956 (2014).

14. Wilson, K. L., Tittensor, D. P., Worm, B. & Lotze, H. K. Incorporating climate change adaptation into marine protected area planning. *Glob. Chang. Biol.* **26**, 3251–3267 (2020).

15. Baums, I. B. *et al.* Considerations for maximizing the adaptive potential of restored coral populations in the western Atlantic. *Ecol. Appl.* **29**, (2019).

16. Matz, M. V., Treml, E. & Haller, B. C. Predicting coral adaptation to global warming in the Indo-West-Pacific. Preprint at *bioRxiv* doi:10.1101/722314 (2019).

17. Selmoni, O., Rochat, E., Lecellier, G., Berteaux-Lecellier, V. & Joost, S. Seascape genomics as a new tool to empower coral reef conservation strategies: an example on north-western Pacific Acropora digitifera. *Evol. Appl.* 588228 (2020). doi:10.1101/588228

18. Riginos, C., Crandall, E. D., Liggins, L., Bongaerts, P. & Treml, E. A. Navigating the currents of seascape genomics: how spatial analyses can augment population genomic studies. *Curr. Zool.* **62**, doi: 10.1093/cz/zow067 (2016).

19. Maina, J., Venus, V., McClanahan, T. R. & Ateweberhan, M. Modelling susceptibility of

551   coral reefs to environmental stress using remote sensing data and GIS models. *Ecol.*
552   *Modell.* **212**, 180–199 (2008).

553   20.   Liu, G., Strong, A. E. & Skirving, W. Remote sensing of sea surface temperatures
554   during 2002 Barrier Reef coral bleaching. *Eos, Trans. Am. Geophys. Union* **84**, 137–141
555   (2003).

556   21.   Rochat, E. & Joost, S. Spatial Areas of Genotype Probability (SPAG): predicting the
557   spatial distribution of adaptive genetic variants under future climatic conditions.
558   Preprint at *bioRxiv* doi:10.1101/2019.12.20.884114 (2019).

559   22.   Boulanger, E., Dalongeville, A., Andrello, M., Mouillot, D. & Manel, S. Spatial graphs
560   highlight how multi-generational dispersal shapes landscape genetic patterns.
561   *Ecography (Cop.).* ecog.05024 (2020). doi:10.1111/ecog.05024

562   23.   Selmoni, O. *et al.* Seascape genomics reveals candidate molecular targets of heat
563   stress adaptation in three coral species. Preprint at *bioRxiv*
564   doi:10.1101/2020.05.12.090050 (2020).

565   24.   Job, S. *Réseau d'Observation des Récifs Coralliens de Nouvelle-Calédonie (RORC)-*
566   *Campagne de suivi 2017-2018*. (2018).

567   25.   Lefèvre, J., Marchesiello, P., Jourdain, N. C., Menkes, C. & Leroy, A. Weather regimes
568   and orographic circulation around New Caledonia. *Mar. Pollut. Bull.* **61**, 413–431
569   (2010).

570   26.   Marchesiello, P., Lefèvre, J., Vega, A., Couvelard, X. & Menkes, C. Coastal upwelling,
571   circulation and heat balance around New Caledonia's barrier reef. *Mar. Pollut. Bull.*
572   **61**, 432–448 (2010).

573   27.   Berkelmans, R., Weeks, S. J. & Steinberga, C. R. Upwelling linked to warm summers
574   and bleaching on the Great Barrier Reef. *Limnol. Oceanogr.* **55**, 2634–2644 (2010).

575   28.   Cravatte, S. *et al.* Regional circulation around New Caledonia from two decades of
576   observations. *J. Mar. Syst.* **148**, 249–271 (2015).

577   29.   Hénin, C., Guillerm, J. & Chabert, L. Circulation superficielle autour de la Nouvelle-
578   Cal{é}donie. *Oc{é}anographie Trop.* **19**, 113–126 (1984).

579   30.   Ayre, D. J. & Hughes, T. P. Genotypic diversity and gene flow in brooding and
580   spawning corals along the great barrier reef, Australia. *Evolution (N. Y).* **54**, 1590–
581   1605 (2000).

582   31.   Magris, R. A., Pressey, R. L., Weeks, R. & Ban, N. C. Integrating connectivity and
583   climate change into marine conservation planning. *Biological Conservation* **170**, 207–
584   221 (2014).

585   32.   Hughes, T. P. *et al.* Global warming transforms coral reef assemblages. *Nature* **556**,
586   492–496 (2018).

587   33.   Welle, P. D., Small, M. J., Doney, S. C. & Azevedo, I. L. Estimating the effect of multiple
588   environmental stressors on coral bleaching and mortality. *PLoS One* **12**, e0175018
589   (2017).

590   34.   Kenkel, C. D., Almanza, A. T. & Matz, M. V. Fine-scale environmental specialization of
591   reef-building corals might be limiting reef recovery in the Florida Keys. *Ecology* **96**,
592   3197–3212 (2015).

593   35.   Palumbi, S. R. Population genetics, demographic connectivity, and the design of
594   marine reserves. *Ecol. Appl.* **13**, 146–158 (2003).

595   36.   Hock, K. *et al.* Connectivity and systemic resilience of the Great Barrier Reef. *PLoS*
596   *Biol.* **15**, (2017).

597   37.   Robinson, J. P. W., Wilson, S. K. & Graham, N. A. J. Abiotic and biotic controls on coral

recovery 16 years after mass bleaching. *Coral Reefs* **38**, 1255–1265 (2019).

38. Kawecki, T. J. Adaptation to Marginal Habitats. *Annu. Rev. Ecol. Evol. Syst.* **39**, 321–342 (2008).

39. Treml, E. A. *et al.* Reproductive output and duration of the pelagic larval stage determine seascape-wide connectivity of marine populations. in *Integrative and Comparative Biology* **52**, 525–537 (2012).

40. Storlazzi, C. D., van Ormondt, M., Chen, Y.-L. & Elias, E. P. L. Modeling Fine-Scale Coral Larval Dispersal and Interisland Connectivity to Help Designate Mutually-Supporting Coral Reef Marine Protected Areas: Insights from Maui Nui, Hawaii. *Front. Mar. Sci.* **4**, 381 (2017).

41. Colberg, F., Brassington, G. B., Sandery, P., Sakov, P. & Aijaz, S. High and medium resolution ocean models for the Great Barrier Reef. *Ocean Model.* **145**, 101507 (2020).

42. Andréfouët, S., Cabioch, G., Flamand, B. & Pelletier, B. A reappraisal of the diversity of geomorphological and genetic processes of New Caledonian coral reefs: A synthesis from optical remote sensing, coring and acoustic multibeam observations. *Coral Reefs* **28**, 691–707 (2009).

43. Dalleau, M. *et al.* Use of habitats as surrogates of biodiversity for efficient coral reef conservation planning in Pacific Ocean islands. *Conserv. Biol.* **24**, 541–552 (2010).

44. Loya, Y. *et al.* Coral bleaching: the winners and the losers. *Ecol. Lett.* **4**, 122–131 (2001).

45. Darling, E. S., Alvarez-Filip, L., Oliver, T. A., McClanahan, T. R. & Côté, I. M. Evaluating life-history strategies of reef corals from species traits. *Ecol. Lett.* **15**, 1378–1386 (2012).

46. EU Copernicus Marine Service. Global Ocean - In-Situ-Near-Real-Time Observations. (2017). Available at: http://marine.copernicus.eu. (Accessed: 2nd February 2017)

47. Merchant, C. J. *et al.* Satellite-based time-series of sea-surface temperature since 1981 for climate applications. *Sci. data* **6**, 223 (2019).

48. UNEP-WCMC, WorldFish-Center, WRI & TNC. Global distribution of warm-water coral reefs, compiled from multiple sources including the Millennium Coral Reef Mapping Project. Version 1.3. (2010). Available at: http://data.unep-wcmc.org/datasets/1. (Accessed: 9th May 2017)

49. QGIS development team. QGIS Geographic Information System. Open Source Geospatial Foundation Project. (2009).

50. Hijmans, R. J. raster: Geographic Data Analysis and Modeling. (2016).

51. R Core Team. R: A Language and Environment for Statistical Computing. (2016).

52. Ryan, W. B. F. *et al.* Global multi-resolution topography synthesis. *Geochemistry, Geophys. Geosystems* **10**, (2009).

53. van Etten, J. gdistance: Distances and Routes on Geographical Grids. (2018). Available at: https://cran.r-project.org/package=gdistance.

54. Kilian, A. *et al.* Diversity arrays technology: A generic genome profiling technology on open platforms. *Methods Mol. Biol.* **888**, 67–89 (2012).

55. Zheng, X. *et al.* A high-performance computing toolset for relatedness and principal component analysis of SNP data. *Bioinformatics* **28**, 3326–3328 (2012).

56. Frichot, E., Schoville, S. D., Bouchard, G. & François, O. Testing for associations between loci and environmental gradients using latent factor mixed models. *Mol. Biol. Evol.* **30**, 1687–1699 (2013).

57. Joost, S. *et al.* A spatial analysis method (SAM) to detect candidate loci for selection: Towards a landscape genomics approach to adaptation. *Mol. Ecol.* **16**, 3955–3969 (2007).

58. Brooks, M. E. *et al.* glmmTMB balances speed and flexibility among packages for zero-inflated generalized linear mixed modeling. *R J.* **9**, 378–400 (2017).

59. Breheny, P. & Burchett, W. Visualization of regression models using visreg. *R J.* **9**, 56–71 (2017).

60. Novembre, J. *et al.* Genes mirror geography within Europe. *Nature* **456**, 98–101 (2008).

61. Patterson, N., Price, A. L. & Reich, D. Population structure and eigenanalysis. *PLoS Genet.* **2**, 2074–2093 (2006).

62. van Oppen, M. J. H., Willis, B. L., Van Rheede, T. & Miller, D. J. Spawning times, reproductive compatibilities and genetic structuring in the Acropora aspera group: Evidence for natural hybridization and semi-permeable species boundaries in corals. *Mol. Ecol.* **11**, 1363–1376 (2002).

63. Schmidt-Roach, S. *et al.* Assessing hidden species diversity in the coral Pocillopora damicornis from Eastern Australia. *Coral Reefs* **32**, 161–172 (2013).

64. Cabreros, I. & Storey, J. D. A likelihood-free estimator of population structure bridging admixture models and principal components analysis. *Genetics* **212**, 1009–1029 (2019).

65. Ferrari, S. L. P. & Cribari-Neto, F. Beta regression for modelling rates and proportions. *J. Appl. Stat.* **31**, 799–815 (2004).

66. Verbeke, G., Molenberghs, G. & Rizopoulos, D. Random effects models for longitudinal data. in *Longitudinal Research with Latent Variables* 37–96 (Springer Berlin Heidelberg, 2010). doi:10.1007/978-3-642-11760-2_2

67. Garcia, T. P. & Marder, K. Statistical Approaches to Longitudinal Data Analysis in Neurodegenerative Diseases: Huntington's Disease as a Model. *Current Neurology and Neuroscience Reports* **17**, 14 (2017).

68. Bozdogan, H. Model selection and Akaike's Information Criterion (AIC): The general theory and its analytical extensions. *Psychometrika* **52**, 345–370 (1987).